

High-resolution experiments on projectile fragments - A new approach to the properties of nuclear matter

A. Kelić¹, M. V. Ricciardi¹, J. Benlliure², M. Bernas³, A. Botvina¹, E. Casarejos², T. Enqvist¹, V. Henzl¹, D. Henzlova¹, P. Napolitani^{1,3}, J. Pereira², K.-H. Schmidt¹, J. Taïeb⁴, O. Yordanov¹

¹GSI, Germany; ²University Santiago de Compostela, Spain; ³IPN-Orsay, France; ⁴CEA, Saclay, France;

Introduction - Dedicated experiments on nucleus-nucleus collisions are the main source of our knowledge on static and dynamic bulk properties of nuclear matter. Most investigations are concentrated on the detection of nucleons, produced particles and very light fragments in full-acceptance experiments. Unfortunately, these results usually reflect the combined influence of static (e.g. incompressibility of nuclear matter) and dynamic properties (e.g. momentum dependence of the nuclear mean field) of nuclear matter. Thus, some ambiguities remain in deducing specific properties of nuclear matter. The need for high-precision information, e.g. a full nuclide identification of preferentially all reaction products and a precise measurement of their momenta is commonly recognized. Since the requirements to achieve large acceptance and high resolution are incompatible in many aspects, experiments with high-resolution magnetic spectrometers, which complement the large-acceptance experiments, represent the optimum solution.

We report on recently performed experiments, which gave access to the excitation of the nucleon in the nuclear medium, to non-local features of the nuclear mean field [1] and to the evolution of the N/Z degree of freedom in nuclear reactions [2].

Experiment - The SIS18 heavy-ion accelerator of GSI was used to provide heavy-ion beams of ^{238}U and ^{208}Pb at 1 A GeV. The beams impinged on four different targets, a $87\text{ mg/cm}^2\ ^1\text{H}$ target, a $208\text{ mg/cm}^2\ ^2\text{H}$ target, a $36\text{ mg/cm}^2\ \text{Ti}$ target, and a $50.5\text{ mg/cm}^2\ \text{Pb}$ target. In the target layers used in these experiments, the primary beam loses less than 1.5% of its energy; thus corrections due to energy loss in the target do not deteriorate the accurate measurement of the longitudinal momenta of the reaction residues. The reaction products entered into the FRS, used as a high-resolution magnetic spectrometer. Full identification in mass and atomic number of the reaction residues was performed by determining the mass-over-charge ratio A/Z from magnetic rigidity and time-of-flight, and by deducing the atomic number Z from an energy-loss measurement with an ionisation chamber. The achieved resolution in mass was around $2.5 \cdot 10^{-3}$, for all measured fragments. Once the reaction residue was identified in mass and atomic number, the measurement of the magnetic rigidity, deduced from the horizontal position at the intermediate dispersive image plane of the FRS, gave precise information on its longitudinal momentum. Because of the limited momentum accep-

tance of the FRS, measurements with different magnetic fields were combined to fully cover the momentum distributions of all residues. In case of the uranium beam, the angular transmission for projectile fragments ranges from 100 % for $A \geq 175$ over more than 90 % for $A = 75$ to about 20 % for $A = 18$. The angular transmission for fission fragments is lower, and amounts to some 10 %. They can only pass the separator when they are emitted close to the forward or backward direction. This can be seen in Fig. 1, which shows two-dimensional cluster plots of the velocity distributions in the projectile frame of the zirconium isotopes from the reaction $^{238}\text{U} + \text{Pb}$, measured at 1 A GeV. Please note that every vertical line of Fig. 1 corresponds to the invariant production cross-section of the presented isotope integrated over the perpendicular velocity in the range corresponding to the momentum acceptance of the FRS.

In Fig. 1, the most neutron-rich isotopes predominantly appear in two narrow velocity ranges, corresponding to fission in forward and backward direction, respectively. The most neutron-deficient isotopes, which are produced by fragmentation, however, are found close to the beam velocity. The separation between fragmentation and fission residues is performed in the present experiments by the pattern in velocity and neutron excess [3], as demonstrated in Fig. 1. In the following, we will consider only the fragmentation residues, with fission events being excluded.

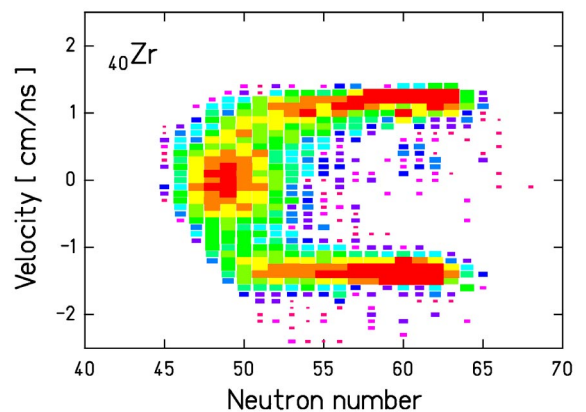


Fig 1. Velocity distributions of ^{40}Zr isotopes produced in the reaction $^{238}\text{U} + \text{Pb}$ at 1 A GeV. The velocities are given in the projectile frame and have been corrected for the energy loss of the projectile and fragments in the target.

The magnetic fields were measured by Hall probes with a relative precision of 10^{-4} . The bending radius was deduced

from the position at the intermediate image plane with a statistical relative uncertainty of $\pm 3 \cdot 10^{-4}$, based on a resolution of ± 2 mm in the position measurement. This results in a relative uncertainty of $\pm 3 \cdot 10^{-4}$ in the momentum of individual reaction products. Details of the experimental set-up and the detector equipment, and a description of the analysis method can be found in references [4,5] and [3,6,7], respectively.

Results

1. Excitation of the nucleon in the nuclear medium. - The momentum distributions of bismuth isotopes, produced by charge-pickup reactions, were determined for the systems $^{208}\text{Pb} + ^{1,2}\text{H}$ at 1 A GeV. Fig. 2 shows the velocity spectrum of the charge-exchange product ^{208}Bi . The high momentum resolution of the FRS allows distinguishing quasielastic collisions of a projectile neutron with a target proton from a transformation of a projectile neutron into a proton via the excitation of a Δ -resonance. The spectra obtained with the two targets show different relative yields for the two processes. They reveal the different characteristics of neutron- and proton-induced collisions with the projectile nucleons.

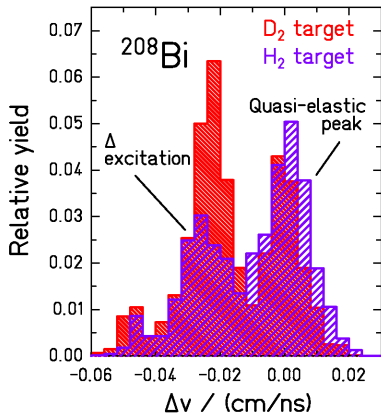


Fig. 2: Velocity distribution, in the projectile frame, of ^{208}Bi formed by charge-exchange from ^{208}Pb projectiles in collisions with protons and deuterons at 1 A GeV.

A quantitative analysis of the momentum distributions and the cross sections to extract the characteristics of Δ excitation in the nuclear medium and a comparison with similar studies for lighter systems [8] is in progress.

2. Momentum dependence of the nuclear mean field - As it was shown in refs. [1,9], also in more central collisions the precise measurement of the kinematical properties of the spectators represents a new tool to determine the in-medium nucleon-nucleon interactions. This method exploits the direct impact of the participants expansion on the kinematical properties of the surviving heavy spectator remnants. According to the model calculations of Shi, Danielewicz and Lacey [9], the peculiar nature of the longitudinal momentum as an observable is the selective sensitivity to the momentum dependence of the mean field. This property is rather unique compared to most experimental signatures,

which are sensitive to both the hardness of the EOS and the momentum dependence of the mean field.

The mean velocities of the spectator residue measured in two reactions, $^{238}\text{U}+\text{Ti}$ and $^{208}\text{Pb}+\text{Ti}$, are shown in Fig. 3 as a function of the final residue mass. These values are corrected for the enhancement of the transmission for fragments with higher velocities. This correction turns out to be very small, it amounts to 0.0003 cm/ns for $A = 162$, to 0.015 cm/ns for $A = 61$, and to 0.035 cm/ns for $A = 40$.

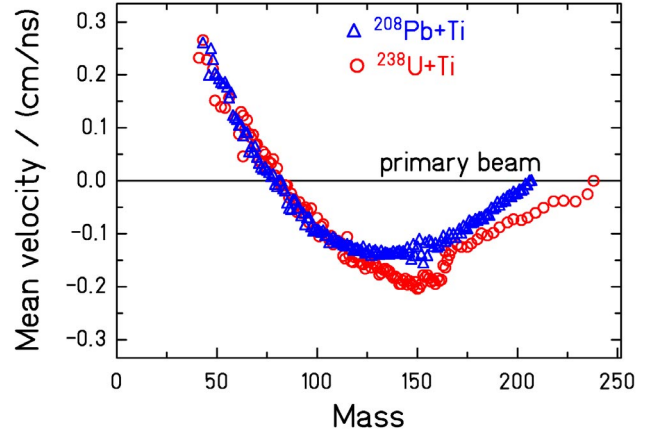


Fig. 3. Mean values of the velocity distributions of reaction residues, excluding fission, produced in $^{238}\text{U} + \text{Ti}$ (squares) and $^{208}\text{Pb} + \text{Ti}$ (triangles) at 1 A GeV in the frame of the projectile.

From Fig. 3 it can be seen that the mean velocity of the heaviest residues, corresponding to the largest impact parameters, decreases with increasing mass loss as given by the Morrissey systematic [10]. On the contrary, for the less peripheral collisions the velocities of the fragmentation products do not decrease any more. The velocities of the lighter fragments even tend to increase, until finally they become even faster than the projectiles.

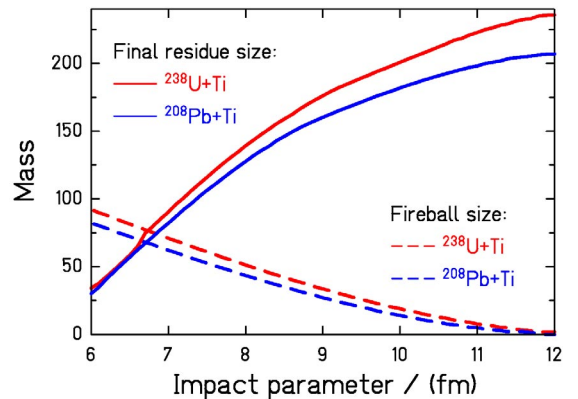


Fig. 4. Mean mass of the final residue (full lines) and size of the fireball (dashed lines) as a function of impact parameter calculated with the abrasion model for the systems $^{238}\text{U} + \text{Ti}$ (in red) and $^{208}\text{Pb} + \text{Ti}$ (in blue) at 1 A GeV.

According to theoretical calculations, this acceleration found for the light reaction residues is a consequence of the

momentum dependence of the nuclear mean field [9]. The magnitude of the effect is rather sensitive to the size of the fireball created. For the mid-peripheral collisions studied here, one expects from the abrasion model [11] that the mass of the final residue is a good measure of the impact parameter. This was experimentally confirmed by data from ALADIN [12]. Calculations with the abrasion model [13] predict that for a given impact parameter, i.e. given spectator-residue mass, the fireball formed in the reactions $^{238}\text{U}+\text{Ti}$ and $^{208}\text{Pb}+\text{Ti}$ has almost the same size, see Fig. 4. Consequently, the acceleration effect observed in these two systems is of similar magnitude. For more quantitative results, detailed comparisons with dedicated theoretical transport calculations are being performed.

3. Isospin thermometer - The study of the properties of nuclear matter with extreme N/Z ratio has come into the focus of recent research activities due to its importance for the understanding of supernova explosions and the stability of neutron stars. Many important results have been obtained by detecting light nuclei ($A \leq 20$) and particles in full-acceptance experiments. Recently, we have shown that valuable information can be obtained by measuring heavier residues produced in mid-peripheral heavy-ion collisions [2]. For the interpretation of such data, the isospin-thermometer method was introduced to determine the freeze-out temperature in fragmentation reactions [2]. According to this method, yields of light fragmentation residues, or more precisely their N/Z ratios, carry the information on the temperature, the system reaches after the break-up. A freeze-out temperature of the order of 5 MeV was deduced from the measured data [2] of the system $^{208}\text{Pb}+\text{Ti}$. In this report we investigate the influence of target and projectile on the evolution of the N/Z of the reaction products. In this context we have analysed the following systems: $^{238}\text{U}+\text{Pb}$ [3], $^{238}\text{U}+\text{Ti}$ [14], $^{208}\text{Pb}+\text{Ti}$ [7], and $^{208}\text{Pb}+^2\text{H}$ [7]. Figure 5 shows an overview of the data on the mean neutron-to-proton ratio $\langle N \rangle / Z$ of the isotopic chains measured for these systems. Several observations can be made. Changing the target, does not have any influence on the N/Z of the fragments: The residues formed by fragmentation of ^{238}U in lead and titanium show the same $\langle N \rangle / Z$; the same is true for the fragmentation of ^{208}Pb . On the contrary, fragments from projectiles with different N/Z are shifted in their $\langle N \rangle / Z$ values: The residues formed by fragmentation of ^{238}U ($N/Z = 1.587$) are slightly more neutron rich than those formed in the fragmentation of ^{208}Pb ($N/Z = 1.537$).

These results confirm the theoretical expectations that there is no isospin diffusion between projectile and target matter in collisions at relativistic energies and that there is a memory of the neutron excess of the projectile found in the projectile fragments, which are far from the projectile. Both results corroborate the basic ideas behind the isospin-thermometer method.

In Fig. 5, the $\langle N \rangle / Z$ values of the light fragments from ^{238}U and ^{208}Pb on Ti at 1 A GeV, are compared with the results of the statistical fragmentation code ABRABLA. The model includes an abrasion stage, where the excited spectator is

formed, and a successive deexcitation phase through an evaporation cascade. In between these two stages, a break-up stage was introduced, where a heavy fragment is formed along with smaller clusters. The result shows that a good agreement with the data is achieved when the break-up stage is taken into account with a freeze-out temperature of 5 MeV. The calculation with a direct abrasion/evaporation model places the final residues on the more neutron-deficient side of the nuclear chart.

Recently it was shown that the break-up stage has to be considered also in the interactions between protons and light nuclei at 1 A GeV [15], what can be essential for better understanding the production mechanisms which create the high-energetic particles that we observe as cosmic rays, but also for the applications in nuclear technology.

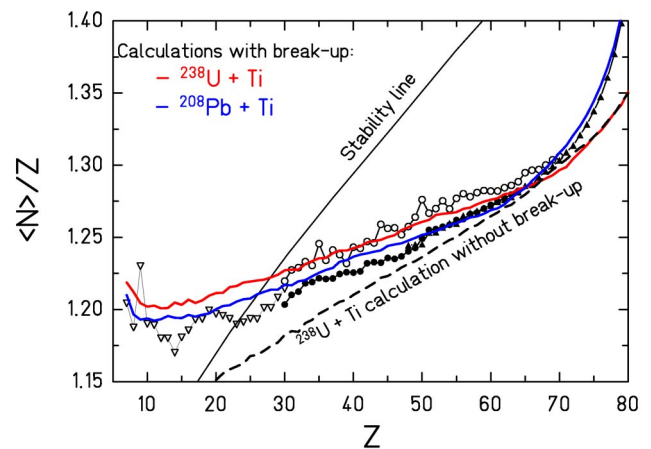


Fig. 5: Experimental $\langle N \rangle / Z$ values from the reactions $^{238}\text{U}+\text{Pb}$ and Ti (open dots and triangles, respectively), and $^{208}\text{Pb}+^2\text{H}$ and Ti (full triangles and full dots, respectively) at 1 A GeV compared with calculations using a statistical fragmentation model. The dashed curve corresponds to a simulation of $^{238}\text{U}+\text{Ti}$ with only abrasion/evaporation stages, the solid curve includes the passage through a break-up phase (red – $^{238}\text{U}+\text{Ti}$, blue – $^{208}\text{Pb}+\text{Ti}$).

- [1] M. V. Ricciardi et al, Phys. Rev. Lett. **90** (2003) 212302.
- [2] K.-H. Schmidt et al., Nucl. Phys. A **710** (2002) 157.
- [3] T. Enqvist et al., Nucl. Phys. A **658** (1999) 47.
- [4] B. Voss et al., Nucl. Instrum. Methods A **364** (1995) 150.
- [5] M. Pfützner et al., Nucl. Instr. Meth. **B 86** (1994) 213.
- [6] M. de Jong et al., Nucl. Phys. A **628** (1998) 479.
- [7] T. Enqvist et al., Nucl. Phys. A **686** (2001) 481.
- [8] C. Gaarde, Annu. Rev. Nucl. Part. Sci. **41** (1991) 187.
- [9] L. Shi et al., Phys. Rev. **C 64** (2001) 034601.
- [10] D. J. Morrissey, Phys. Rev. **C 39** (1989) 460.
- [11] L. F. Oliveira et al., Phys. Rev. **C 19** (1979) 826.
- [12] J. Hubele et al., Z. Phys. A **340** (1991) 263.
- [13] J.-J. Gaimard et al., Nucl. Phys. A **531** (1991) 709.
- [14] M. V. Ricciardi, GSI, PhD Thesis - in progress.
- [15] P. Napolitani et al., Proc of IMW2003, Caen (France), 2003.